Int J Clin Exp Med 2019;12(2):1897-1905
www.ijcem.com /ISSN:1940-5901/IJCEM0078147

Original Article

Texture analysis based on intravoxel incoherent motion DWI for stratification of the clinical stages of nasopharyngeal cancer

Jing Hou[1,2], Yuhui Qin[1], Ying Hu[3], Feiping Li[1], Lu Wen[1], Qiang Lu[1], Wenbin Zeng[2], Xiaoping Yu[1]

[1]Department of Diagnostic Radiology, Hunan Cancer Hospital and The Affiliated Cancer Hospital of Xiangya School of Medicine, Central South University, 283 Tongzipo Road, Yuelu District, Changsha 410013, Hunan, P. R. China; [2]School of Pharmaceutical Sciences, Central South University, Changsha 410013, Hunan, P. R. China; [3]Department of Radiotherapy, The Affiliated Cancer Hospital of Xiangya School of Medicine, Central South University, Changsha 410013, Hunan, P. R. China

Received April 18, 2018; Accepted October 30, 2018; Epub February 15, 2019; Published February 28, 2019

Abstract: The objective of the study was to investigate the utility of texture analysis based on intravoxel incoherent motion diffusion-weighted imaging (IVIM-DWI) for stratifying the clinical stages of nasopharyngeal cancer (NPC). Ninety NPC patients were stratified into low and high clinical stage groups based on the American Joint Committee on Cancer (AJCC) and TNM staging system. Texture features of the primary NPC lesion were extracted from IVIM-DWI parametric maps. The Fisher coefficient (Fisher), probability of classification error and average correlation (POE+ACC), mutual information coefficients (MI), and the combination of the above three methods (FPM) were applied to select texture features. Subsequently, each texture feature subset was analyzed via raw data analysis (RDA), principal component analysis (PCA), linear discriminant analysis (LDA) and nonlinear discriminant analysis (NDA), and the misclassification probability in stratifying the NPC clinical stages was calculated correspondingly. The best discrimination of the AJCC stage of NPC was obtained with the *f* map and the FPM method combined with NDA classifier, which had the lowest misclassification probability of 1.25%. The best discrimination of T stage was obtained with the FPM method combined with NDA classifier of the ADC or *f* map, which had equal lowest misclassification probabilities of 9.03%. The best separation of the N stage was also obtained with the FPM method combined with the NDA classifier of the ADC map, which had the lowest misclassification probability of 1.25%. Significant differences were observed in the lowest misclassification probability with the four classification methods, but not with the four IVIM-DWI parametric maps in predicting the AJCC, T and N stages. Texture analysis based on IVIM-DWI may be valuable in the pretreatment stratification of NPC clinical stages, and the FPM feature selection method combined with NDA classifier may provide the best discrimination performance.

Keywords: Nasopharyngeal carcinoma, texture analysis, clinical stage, intravoxel incoherent motion, diffusion weighted imaging

Introduction

Nasopharyngeal carcinoma (NPC) is one of the most common malignancies in Southern China and Southeast Asia, with a reported incidence of 15/100,000 to 24/100,000 populations per year [1]. Due to the complex anatomical structures of the nasopharynx, most newly diagnosed NPCs tend to present with an advanced disease. Although chemoradiotherapy (CRT) is the standard treatment for NPC, not all patients respond well to CRT. Accurate pretreatment staging to distinguish between low-stage and high-stage NPC is of paramount importance in devising the optimal and personalized treatment regime.

Magnetic resonance imaging (MRI) is widely used in clinical practice for determining the initial diagnosis and clinical stage of NPC. In recent years, functional MRI (fMRI), including dynamic contrast enhancement magnetic resonance imaging (DCE-MRI) and diffusion-weighted imaging (DWI), has been increasingly applied for characterizing NPC [2-5]. However, most of the recently published literature on NPC is

based on the quantitative analysis of the mean value of fMRI parameters usually within a largest cross-sectional region of interest (ROI) on MRI images, which neglects the heterogeneity of tumors. Heterogeneity is an extremely important histological feature of malignancies and is linked to tumor malignancy degree and aggressiveness [6, 7]. A study [8] on esophageal cancer by B. Ganeshan et al. reported that tumor heterogeneity was greater in patients with clinical stages III or IV than in those with stage II. Texture analysis, one of the "radiomics" approaches, is a quantitative image processing algorithm that can quantify tissue heterogeneity by evaluating the distribution of texture irregularity and coarseness within a lesion [9]. It is thus expected to allow a more quantitative and detailed evaluation of the lesion characteristics than the mean value of fMRI parameters. Several studies have demonstrated the potential of texture analysis for staging rectal cancer [10], non-small cell lung cancer [11], esophageal cancer [8], renal cell carcinoma [12] and parotid gland lesions [13].

However, to date, most of the recently published studies on MRI-based texture analysis made use of morphological maps, and a few were based on mono-exponential ADC maps. The former cannot reflect functional information of tissues, including diffusion and perfusion. The latter only reflects hybrid diffusion information and thus cannot accurately provide the diffusion information. Intravoxel incoherent motion DWI (IVIM-DWI), a new DWI technique, was proposed to separate the true diffusion due to Brownian movement from the pseudo-diffusion caused by microcirculatory perfusion of blood within capillaries in tissues [14]. Recently, IVIM-DWI was shown to be a more accurate tool than conventional DWI in characterizing NPC [15] and other tumors [16, 17]. Moreover, a study by Vincent Lai et al. [3] explored the relationship of the diffusion and perfusion characteristics derived from IVIM-DWI to the clinical stages of NPC, which demonstrated the potential of IVIM-DWI in pretreatment staging for NPC. Therefore, we speculate that texture analysis based on IVIM-DWI may provide more information and may be more valuable in stratifying the clinical stages of NPC. Thus, the purpose of this study was to explore the efficacy of texture features derived from IVIM-DWI in stratifying the clinical stages of NPC.

Materials and methods

Patient selection

This prospective study was approved by the Medical Ethics Committee at our institution, and all NPC patients signed written informed consent. The inclusion criteria of this study were as follows: (1) newly diagnosed and pathologically confirmed of nonkeratinizing NPC, (2) age above 18 years, and (3) Karnofsky score ≥80. Patients were excluded if they (1) had prior anti-tumor treatment for NPC, (2) did not sign the informed consent form, or (3) had contraindications for MRI.

All patients' clinical stages were determined by two head and neck radiologists (Y.X and W.L with 20 and 5 years in radiology, respectively) with reference to the 7 th edition of the International Union Against Cancer/American Joint Committee on Cancer (UICC/AJCC) staging system after department discussion and consensus based on the MRI examinations of the head and neck, computed tomography (CT) scan of the chest, and MRI examination and/or nuclear medicine examination of the other parts of the body.

Conventional MRI protocols

All MRI examinations were performed on a 1.5 Tesla MRI scanner (Optima® MR360, GE Healthcare, Milwaukee, WI, USA) using a head and neck coil for all NPC patients at baseline. The conventional MRI protocols included axial T1-weighted spin-echo images (repetition time [TR]/echo time [TE] 580 ms/7.8 ms, 5 mm slice thickness, 1 mm slice gap, and number of excitations [NEX] 2) and axial T2-weighted spin-echo images with fat suppression (TR/TE 6289 ms/85 ms, 5 mm section thickness, 1 mm slice gap, and 2 NEX).

IVIM-DWI protocol

An IVIM-DWI examination was also performed on all NPC patients at baseline. Ten b-values (0, 50, 80, 100, 150, 200, 400, 600, 800 and 1000 s/mm^2) were applied with a single-shot diffusion-weighted spin-echo echo-planar (SE-DW-EPI) sequence. The lookup table for gradient directions was modified to allow multiple b value measurements in one series. Parallel imaging was used with an acceleration factor of 2.

A local shim box covering the nasopharyngeal region was applied to minimize susceptibility artifacts. In total, 12 axial slices covering the nasopharynx were obtained with a 22 cm field of view, 5 mm slice thickness, 1 mm slice gap, 4225 ms TR, 106 ms TE, 128 × 130 matrix, and 4 NEX.

IVIM-DWI parametric maps acquisition

All IVIM-DWI data were transferred to an Advantage Workstation with Functool software (version AW 4.6, GE Medical Systems) for post-processing. The MADC kit, a software package for multiple ADC measurement in the Functool software package, was performed for the IVIM-DWI analysis. The ADC, D, D^* and *f* maps of each NPC patient were generated on the basis of a pixel-by-pixel fitting according to the Levenberg-Marquardt algorithm [18]. For IVIM fitting, two-step fitting was applied to increase the fitting robustness. A constrained sequential model was used in the fitting of the data for the IVIM model. Subsequently, these maps were saved as BMP format images for texture analysis.

Texture analysis

The abovementioned BMP format images were loaded into the MaZda (http://www.eletel.p.lodz.pl/programy/mazda/index.php? action=mazda) program for texture analysis. The main steps of the texture analysis were as follows.

ROI selection

Three-dimensional (3D) volume of interest (VOI) analysis based on the IVIM-DWI parametric maps was applied in this study. On the two-dimensional (2D) main window of MaZda software, one radiologist (H.J. with five years of experience in head and neck MRI) who was blinded to the clinical data of the subjects manually delineated an ROI, which included the lesion on its ADC, D, D^* and *f* maps, just inside the outer margin of the lesion to minimize the partial volume error. Both the most superior and the most inferior slices for each tumor were excluded to avoid volume averaging. Subsequently, with the 3D editor window, the above-selectemd cross-sections were updated, and a VOI of the tumor was generated automatically. For each VOI, gray-level normalization was performed using $\mu \pm 3\sigma$ (μ, gray-level mean; σ, gray-level standard deviation) to minimize the influence of contrast and brightness variation. Texture features of the VOIs were automatically calculated by the MaZda software.

Feature extraction

Texture analysis yielded 279 texture features, including 9 histogram-based features, 5 gradient-based features, 11 co-occurrence matrix-based features derived from 20 co-occurrence matrices produced for 4 directions and 5 inter-pixel distances, 5 run-length matrix-based features in 4 different directions each, 5 autoregressive model-based features, and 20 Haar wavelet transform-based features. Briefly, histogram-based features belong to the first-order histogram features. These features describe the histogram of the signal intensity values of voxels within the VOI, including the mean, variance, skewness, kurtosis and percentiles. Gradient-based features use the histogram of the image's absolute gradient values to describe the image intensity distribution. The co-occurrence matrix is a second order histogram calculated from the intensities of pairs of voxels to define the spatial relationship of the pairs of voxels. Run-length matrix features refer to the length, frequency and uniformity of runs of similar voxel intensity values in different directions in the VOI. The co-occurrence matrix and run-length matrix are calculated in four directions. The autoregressive model assumes a local interaction between image voxels, in that the voxel intensity is a weighted sum of four neighboring voxel intensities. The model parameters can be estimated by minimizing the sum of the squared error. Finally, the Harr wavelet transform features describe the wavelet transform of the voxels in the VOI and summarize the frequency of similar signal intensities in the VOI.

Feature selection

Selection of texture features was performed automatically by using four selection methods provided by MaZda. The first is based on the Fisher coefficient (Fisher) (ratio of between-class to within-class variance), the second uses both the minimization of classification error probability and the average correlation coefficients (POE+ACC), the third implements the mutual information coefficient (MI), which measure the dependence between two or more random variables' coefficients, and the fourth com-

Table 1. Misclassification probability of AJCC stage

Parameters	Feature selection methods	Classifiers			
		RDA	PCA	LDA	NDA
ADC	Fisher	11.25%	12.36%	15.27%	5.00%
	POE+ACC	13.89%	15.97%	14.58%	2.5%
	MI	15.27%	16.67%	14.44%	8.33%
	FPM	16.38%	16.38%	13.19%	8.33%
D	Fisher	19.44%	19.16%	15.83%	8.75%
	POE+ACC	16.25%	17.50%	17.78%	3.75%
	MI	17.78%	16.38%	12.5%	2.5%
	FPM	15.56%	15.56%	11.25%	2.5%
D*	Fisher	18.75%	16.94%	16.66%	8.33%
	POE+ACC	20.83%	17.36%	15.28%	2.5%
	MI	18.75%	18.47%	13.19%	8.33%
	FPM	18.19%	17.36%	11.25%	3.75%
f	Fisher	13.88%	15.28%	13.88%	3.75%
	POE+ACC	15.97%	18.05%	12.5%	5.56%
	MI	16.66%	13.19%	15.28%	2.50%
	FPM*	19.44%	15.97%	6.94%	1.25%

Note: AJCC: American Joint Committee on Cancer. ADC: apparent diffusion coefficient. D*: pseudo-diffusion coefficient. D: pure diffusion coefficient. *f*: perfusion fraction. RDA: raw data analysis. PCA: principal component analysis. LDA: linear discriminant analysis. NDA: nonlinear discriminant analysis. Fisher: Fisher coefficient. POE+ACC: classification error probability combined with average correlation coefficients. MI: mutual information coefficient. FPM: the combination of Fisher, POE+ACC, and MI. *: Chi-square test was performed to compare the misclassification probability of the four classifiers for *f* map (x^2=16.926, P<0.0001).

bines the aforementioned three methods (FPM) [9, 19]. Each of the first three methods can choose a subset consisting of 10 optimal texture features, and the FPM can select a subset including 30 optimal texture features. These methods were used to obtain the most significant texture features for stratifying the clinical stages of NPC.

Data analysis and classification

The subsets of selected texture features were set as an input in an integrated module B11 application (version 4.6) for data analysis and classification in the MaZda software. Raw data analysis (RDA), principal component analysis (PCA), linear discriminant analysis (LDA) and nonlinear discriminant analysis (NDA) provided by the B11 module were performed for each subset of texture features, and the minimum error probability of each classification was calculated. Nearest-neighbor (1-NN) classification was performed for the RDA. The most expressive features (MEF) and the most discriminating features (MDF) resulted from the PCA and LDA, respectively. The NDA performed the classification of the texture features via an artificial neural network (ANN). These classification procedures with RDA, PCA, LDA, and NDA were automatically run by B11.

Statistical analysis

Statistical analyses were performed with SPSS version 22.0 (SPSS Inc, Chicago, IL), MedCalc v15.0 software (MedCalc Software bvba, Ostend, Belgium) and MaZda software. Differences were considered significant if the P value was less than 0.05. First, the misclassification probabilities of the combination of four IVIM-DWI parameters, four feature selection methods and four classifiers in stratifying the AJCC, T and N stages were calculated automatically by MaZda software as mentioned above. Next, 10-fold cross-validation was performed to further test the reliability of the feature selection methods and classifiers in terms of their performances in stratifying nasopharyngeal cancer clinical stage. Then, four lowest misclassification probabilities corresponding to four IVIM-DWI parameters in stratifying the AJCC, T and N stages were calculated respectively. A chi-square test was performed to investigate significant differences in the lowest misclassification probability of the four IVIM-DWI parameters respectively. Moreover, the lowest one was chosen among the four as the lowest misclassification probability in stratifying the AJCC, T and N stages. Subsequently, a chi-square test was performed to investigate significant differences between the misclassification probability of the classifier calculating the lowest misclassification probability and the other three classifers.

Results

Clinical characteristics of the study participants

From September 2016 to April 2017, 99 consecutive patients were initially recruited. Of the 99 initially enrolled patients, 9 were eliminated from this study because of serious image dis-

Table 2. Misclassification probability of T stage

Parameters	Feature selection methods	Classifiers			
		RDA	PCA	LDA	NDA
ADC	Fisher	48.61%	45.83%	46.52%	18.05%
	POE+ACC	59.72%	56.94%	40.27%	19.44%
	MI	38.19%	43.05%	38.89%	17.36%
	FPM#	34.72%	35.41%	29.17%	9.03%
D	Fisher	53.47%	55.56%	26.39%	17.12%
	POE+ACC	48.61%	52.78%	48.61%	21.52%
	MI	54.16%	56.12%	35.13%	18.33%
	FPM	54.86%	52.11%	36.11%	10.41%
D*	Fisher	48.61%	48.99%	36.11%	21.52%
	POE+ACC	57.08%	59.72%	39.58%	18.75%
	MI	56.94%	49.31%	47.91%	27.63%
	FPM	36.81%	38.89%	27.78%	10.14%
f	Fisher	58.19%	56.94%	35.97%	17.36%
	POE+ACC	49.55%	54.76%	47.22%	19.31%
	MI	51.38%	50.69%	37.22%	21.11%
	FPM*	56.25%	59.02%	27.08%	9.03%

Note: ADC: apparent diffusion coefficient. D*: pseudo-diffusion coefficient. D: pure diffusion coefficient. *f*: perfusion fraction. RDA: raw data analysis. PCA: principal component analysis. LDA: linear discriminant analysis. NDA: nonlinear discriminant analysis. Fisher: Fisher coefficient. POE+ACC: classification error probability combined with average correlation coefficients. MI: mutual information coefficient. FPM: the combination of Fisher, POE+ACC, and MI. #: Chi-square test was performed to compare the misclassification probability of the four classifications for ADC map (x^2=14.706, P=0.0001). *: Chi-square test was performed to compare the misclassification probability of the four classifiers for *f* map (x^2=51.354, P<0.0001).

tortion (n=4), dental artifacts (n=3), or withdrawal by patients (n=2). The remaining 90 patients (62 males, 28 females; mean age: 49.24±12.07 years; age range: 18-70 years) were stratified into two groups: the low- and high-stage groups. Patients with an AJCC stage of I (n=1) or II (n=6), T stage of T1 (n=9) or T2 (n=31), or N stage of N0 (n=5) or N1 (n=8) were correspondingly classified into the low-stage groups of AJCC, T and N stage, respectively. Patients with an AJCC stage of III (n=44) or IV (n=39), T stage of T3 (n=27) or T4 (n=23), or N stage of N2 (n=58) or N3 (n=19) were categorized into the high-stage groups of AJCC, T and N stage, respectively. Classification of the M stage was not investigated in this study because of the small cohort with stage M1 (n=2).

Classification of clinical stages

According to a 10-fold cross-validation test, the best discrimination of the AJCC stage of NPC was obtained for the *f* map with the FPM method combined with NDA classifier, which had the lowest misclassification probability of 1.25% compared with the values for the other three classifiers (x^2=16.926, P< 0.0001). The best distinguisher of the T stage was with the FPM method combined with NDA classifier of the ADC or *f* maps, which had equal lowest misclassification probabilities of 9.03% which were lower than those of the other three classifiers (x^2=14.706, P=0.0001; x^2=51.354, P<0.0001, respectively). The best separation of the N stage was also obtained with the FPM method combined with NDA classifier of the ADC map, which had the lowest misclassification probability of 1.25% among those of the other three classifiers (x^2= 11.976, P=0.0005). No significant differences were found in the lowest misclassification probability of the four IVIM-DWI parametric maps in predicting the AJCC (x^2= 0.263, P=0.6081), T (x^2=0.147, P= 0.986) or N (x^2=1.108, P=0.2925) stages in patients with NPC. The misclassification probability of different IVIM-DWI parameters, feature selection methods and classifiers in the classification of AJCC, T and N stages are shown in **Tables 1**-**3**, respectively. Two NPC patients from the low (II) and high (IVa) AJCC groups are shown in **Figure 1**.

Discussion

The clinical stage has been shown to be vital for treatment and prognosis in NPC [20, 21]. Our study demonstrates that texture analysis based on IVIM-DWI is feasible for stratifying the clinical stages of NPC, with a low error probability. Furthermore, the FPM feature selection method combined with the NDA classifier model obtained the best discrimination for the AJCC, T and N stages of NPC.

To our knowledge, most of the previous studies on texture analysis in cancers relied on 2D ROIs that were placed inside a tumor at the largest cross-sectional area. Although this approach is simple and practical, it has some limitations

Table 3. Misclassification probability of N stage

Parameters	Feature selection methods	Classifiers			
		RDA	PCA	LDA	NDA
ADC	Fisher	26.38%	22.22%	19.44%	13.19%
	POE+ACC	21.52%	19.72%	25.00%	13.89%
	MI	22.91%	23.61%	20.83%	7.64%
	FPM#	18.75%	21.53%	15.28%	1.25%
D	Fisher	26.94%	28.47%	27.36%	6.94%
	POE+ACC	24.31%	21.11%	27.78%	9.03%
	MI	21.81%	21.52%	20.55%	14.58%
	FPM	30.56%	29.03%	10.41%	5.56%
D*	Fisher	27.08%	26.67%	24.86%	9.03%
	POE+ACC	26.39%	21.94%	22.08%	3.47%
	MI	24.44%	24.86%	22.91%	3.33%
	FPM	37.50%	37.22%	8.19%	3.47%
f	Fisher	21.39%	21.94%	27.08%	15.13%
	POE+ACC	19.30%	16.67%	26.80%	13.89%
	MI	22.08%	28.33%	23.89%	4.58%
	FPM	21.39%	18.47%	17.36%	4.44%

Note: ADC: apparent diffusion coefficient. D*: pseudo-diffusion coefficient. D: pure diffusion coefficient. *f*: perfusion fraction. RDA: raw data analysis. PCA: principal component analysis. LDA: linear discriminant analysis. NDA: nonlinear discriminant analysis. Fisher: Fisher coefficient. POE+ACC: classification error probability combined with average correlation coefficients. MI: mutual information coefficient. FPM: the combination of Fisher, POE+ACC, and MI. #: Chi-square test was performed to compare the misclassification probability of the four classifiers for ADC map (x^2=11.976, *P*=0.0005).

caused by the variations in ROI positioning and size. The tumor is spatially heterogeneous. Some studies [22, 23] have demonstrated that whole-tumor (3D VOI) analysis can better reflect tumor heterogeneity and is more accurate in characterizing colorectal cancer than the single-section ROI (2D ROI) method. Another study also revealed that 3D VOI texture analysis based on a co-occurrence matrix achieved better discrimination of the solid component of glioma from tumor necrosis and edema than did the 2D method of analyzing T1-weighted MR images. The 3D method was reportedly able to characterize tumor heterogeneities more correctly [24]. Therefore, in this present study, whole-tumor-based analysis was applied for stratifying the clinical stages of NPC.

Texture analysis is based on imaging, but b-e yond imaging. By converting medical images into quantitative imaging features, texture analysis can extract more quantitative information than visual observation [25]. In this study, four feature selection methods (Fisher, POE+ACC, MI and FPM) and four classification analysis methods (RDA, PCA, LDA and NDA) were applied. It was found that there were significant differences in the performance of the cross-combinations of the four feature selection methods and four classification methods in classifying the clinical stages of NPC. First, no matter which IVIM-derived parameter or feature selection method was chosen, the NDA classifier obtained the lowest misclassification probability compared with those of the other three classifiers in stratifying the AJCC, T and N stages of NPC in this study. It is noted that the RDA, PCA and LDA classification methods are based on linear analysis, whereas the NDA classifier is based on an artificial neural network. An artificial neural network is believed to be a more reliable and efficient algorithm with a greater predictive power than linear analyses including RDA, PCA and LDA [26]. Several studies also showed that NDA achieved higher classification accuracy than LDA did in multiple sclerosis [27], brain tumor [26, 28, 29] and non-Hodgkin lymphoma [19]. Furthermore, among the four feature selection methods and the four classification methods in this study, the FPM feature selection method combined with the NDA classifier obtained the best discrimination of the AJCC, T and N stages, with a very low misclassification probability (1.25%, 9.03% and 1.25%, respectively).

With the four IVIM-DWI parameters, the present study demonstrated the lowest misclassification probability in predicting the AJCC stage with *f*, in predicting the T stage with ADC or *f*, and in predicting the N stage with ADC. However, no statistically significant differences were found in the lowest misclassification probability obtained with the four IVIM-DWI parametric maps in predicting the AJCC, T and N stages of NPC, which illustrated that texture analyses based on diffusion and on perfusion parametric maps are equally useful for predicting the clinical stage of NPC. It is of note that the lowest misclassification probability for stratifying

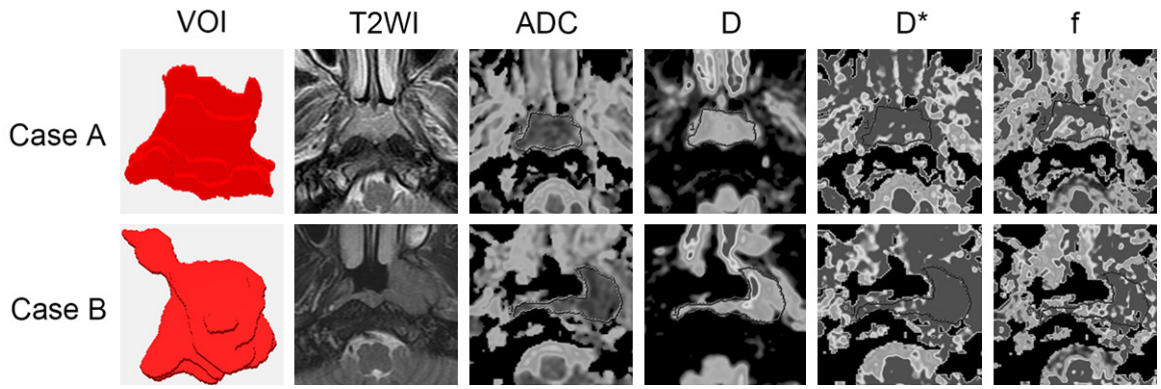

Figure 1. Examples of IVIM-DWI, VOI for texture features extraction, and T2WI for nasopharyngeal carcinoma. The upper row shows images from a patient of low AJCC stage (II) (Case A), whereas the lower row exhibits images from a patient of high AJCC stage (IVa) (Case B).

the T stage is higher than those for the AJCC and N stages, which may be explained by the fact that the T stage of NPC is mainly determined by anatomic and morphologic factors and is only slightly influenced by function information, such as diffusion and perfusion.

One of the limitations existing in the present study is that we ran the feature selection and classification procedures with the same cohort because of the relatively limited data. Larger data sets are needed to run feature selection and classification with training datasets, and to test the performance of feature selection methods and classification methods in validation datasets. In addition, the VOIs were manually delineated and measured by only a single operator, a process that may be subject to interobserver variability. However, because most of the recently used texture features are based on spatial averaging, these features are not very sensitive to small differences in the delineation of VOIs [28].

In conclusion, texture analysis based on IVIM-DWI parametric maps may be valuable in the pretreatment stratification of NPC clinical stage, and the FPM feature selection method combined with the NDA classifier may provide the best discrimination performance.

Acknowledgements

This study was supported by the Provincial Key Clinical Specialty (Medical Imaging) Development Program from Health and Family Planning Commission of Hunan Province, China (contract grant number: 2015/43), and by the Guidance Program for Clinical Technique Innovation from Provincial Science and Technology Department, Hunan, China (project number: 2017SK50601). We would like to show our gratitude to Mr. Zhang Zhong-ping (GE Healthcare China, Beijing, People's Republic of China) for his assistance in MRI analysis.

Disclosure of conflict of interest

None.

Address correspondence to: Xiaoping Yu, Department of Diagnostic Radiology, Hunan Cancer Hospital and The Affiliated Cancer Hospital of Xiangya School of Medicine, Central South University, 283 Tongzipo Road, Yuelu District, Changsha 410013, Hunan, P. R. China. Tel: +86 13607313419; Fax: +86 731 89762577; E-mail: nj9015@163.com

References

[1] Peng H, Chen L, Zhang Y, Li WF, Mao YP, Liu X, Zhang F, Guo R, Liu LZ, Tian L, Lin AH, Sun Y and Ma J. The tumour response to induction chemotherapy has prognostic value for long-term survival outcomes after intensity-modulated radiation therapy in nasopharyngeal carcinoma. Sci Rep 2016; 6: 24835-24843.

[2] Huang B, Wong CS, Whitcher B, Kwong DL, Lai V, Chan Q, Khong PL. Dynamic contrast-enhanced magnetic resonance imaging for characterising nasopharyngeal carcinoma: comparison of semiquantitative and quantitative parameters and correlation with tumour stage. Eur Radiol 2013; 23: 1495-1502.

[3] Lai V, Li X, Lee VH, Lam KO, Fong DY, Huang B, Chan Q, Khong PL. Nasopharyngeal carcinoma: comparison of diffusion and perfusion

characteristics between different tumour stages using intravoxel incoherent motion MR imaging. Eur Radiol 2014; 24: 176-183.
[4] Chen YB, Liu XY, Zheng DC, Xu LY, Hong L, Xu Y and Pan JJ. Diffusion-weighted magnetic resonance imaging for early response assessment of chemoradiotherapy in patients with nasopharyngeal carcinoma. Magn Reson Imaging 2014; 32: 630-637.
[5] Zheng DC, Chen YB, Chen Y, Xu LY, Lin FJ, Lin J, Huang CB and Pan JJ. Early assessment of induction chemotherapy response of nasopharyngeal carcinoma by pretreatment diffusion-weighted magnetic resonance imaging. J Comput Assist Tomogr 2013; 37: 673-680.
[6] Jackson A, O'Connor JP, Parker GJ, Jayson GC. Imaging tumor vascular heterogeneity and angiogenesis using dynamic contrast-enhanced magnetic resonance imaging. Clin Cancer Res 2007; 13: 3449-3459.
[7] Jansen JF, Koutcher JA, Shukla-Dave A. Non-invasive imaging of angiogenesis in head and neck squamous cell carcinoma. Angiogenesis 2010; 13: 149-160.
[8] Ganeshan B, Skogen K, Pressney I, Coutroubis D and Miles K. Tumour heterogeneity in oesophageal cancer assessed by CT texture analysis: preliminary evidence of an association with tumour metabolism, stage, and survival. Clin Radiol 2012; 67: 157-164.
[9] Materka A. Texture analysis methodologies for magnetic resonance imaging. Dialogues Clin Neurosci 2004; 6: 243-250.
[10] Liang CS, Huang YQ, He L, Chen X, Ma Z, Dong D, Tian J, Liang CH and Liu ZY. The development and validation of a CT-based radiomics signature for the preoperative discrimination of stage I-II and stage III-IV colorectal cancer. Oncotarget 2016; 7: 31401-31412.
[11] Ganeshan B, Abaleke S, Young RC, Chatwin CR and Miles KA. Texture analysis of non-small cell lung cancer on unenhanced computed tomography: initial evidence for a relationship with tumour glucose metabolism and stage. Cancer Imaging 2010; 10: 137-143.
[12] Kierans AS, Rusinek H, Lee A, Shaikh MB, Triolo M, Huang WC and Chandarana H. Textural differences in apparent diffusion coefficient between low-and high-stage clear cell renal cell carcinoma. AJR Am J Roentgenol 2014; 203: 637-644.
[13] Fruehwald-Pallamar J, Czerny C, Holzer-Fruehwald L, Nemec SF, Mueller-Mang C, Weber M and Mayerhoefer ME. Texture-based and diffusion-weighted discrimination of parotid gland lesions on MR images at 3.0 Tesla. NMR Biomed 2013; 26: 1372-1379.
[14] Le Bihan D, Breton E, Lallemand D, Aubin ML, Vignaud J and Laval-Jeantet M. Separation of diffusion and perfusion in intravoxel incoherent motion MR imaging. Radiology 1988; 168: 497-505.
[15] Xiao-ping Y, Jing H, Fei-ping L, Yin H, Qiang L, Lanlan W and Wei W. Intravoxel incoherent motion MRI for predicting early response to induction chemotherapy and chemoradiotherapy in patients with nasopharyngeal carcinoma. J Magn Reson Imaging 2016; 43: 1179-1190.
[16] Ganten MK, Schuessler M, Bauerle T, Muenter M, Schlemmer HP, Jensen A, Brand K, Dueck M, Dinkel J, Kopp-Schneider A, Fritzsche K and Stieltjes B. The role of perfusion effects in monitoring of chemoradiotherapy of rectal carcinoma using diffusion-weighted imaging. Cancer Imaging 2013; 13: 548-556.
[17] Lu YG, Jansen JF, Stambuk HE, Gupta G, Lee N, Gonen M, Moreira A, Mazaheri Y, Patel SG, Deasy JO, Shah JP and Shukla-Dave A. Comparing primary tumors and metastatic nodes in head and neck cancer using intravoxel incoherent motion imaging: a preliminary experience. J Comput Assist Tomogr 2013; 37: 346-352.
[18] Marquardt D. An algorithm for least-squares estimation of nonlinear parameters. SIAM J Appl Math 1963; 11: 431-441.
[19] Harrison L, Dastidar P, Eskola H, Jarvenpaa R, Pertovaara H, Luukkaalarg T, Kellokumpu-Lehtinen PL and Soimakallio S. Texture analysis on MRI images of non-Hodgkin lymphoma. Comput Biol Med 2008; 38: 519-524.
[20] Chua DT, Sham JST, Wei WI, Ho WK and Au GKH. The predictive value of the 1997 American joint committee on cancer stage classification in determining failure patterns in nasopharyngeal carcinoma. Cancer 2001; 92: 2845-2855.
[21] Wei WI and Mok VW. The management of neck metastases in nasopharyngeal cancer. Curr Opin Otolaryngol Head Neck Surg 2007; 15: 99-102.
[22] Goh V, Halligan S, Gharpuray A, Wellsted D, Sundin J and Bartram CI. Quantitative assessment of colorectal cancer tumor vascular parameters by using perfusion CT: influence of tumor region of interest. Radiology 2008; 247: 726-732.
[23] Lambregts DM, Beets GL, Maas M, Curvo-Semedo L, Kessels AG, Thywissen T and Beets-Tan RG. Tumour ADC measurements in rectal cancer: effect of ROI methods on ADC values and interobserver variability. Eur Radiol 2011; 21: 2567-2574.
[24] Mahmoud-Ghoneim D, Toussaint G, Constans JM and de Certaines JD. Three dimensional texture analysis in MRI: a preliminary evaluation in gliomas. Magn Reson Imaging 2003; 21: 983-987.

[25] Huang XW, Zhang YL, Qian M, Meng L, Xiao Y, Niu LL, Zheng RQ and Zheng HR. Classification of carotid plaque echogenicity by combining texture features and morphologic characteristics. J Ultrasound Med 2016; 35: 2253-2261.
[26] Orphanidou-Vlachou E, Vlachos N, Davies NP, Arvanitis TN, Grundy RG and Peet AC. Texture analysis of T1-and T2-weighted MR images and use of probabilistic neural network to discriminate posterior fossa tumours in children. NMR Biomed 2014; 27: 632-639.
[27] Harrison LC, Raunio M, Holli KK, Luukkaala T, Savio S, Elovaara I, Soimakallio S, Eskola HJ and Dastidar P. MRI texture analysis in multiple sclerosis: toward a clinical analysis protocol. Acad Radiol 2010; 17: 696-707.
[28] Georgiadis P, Cavouras D, Kalatzis I, Daskalakis A, Kagadis GC, Sifaki K, Malamas M, Nikiforidis G and Solomou E. Improving brain tumor characterization on MRI by probabilistic neural networks and non-linear transformation of textural features. Comput Methods Programs Biomed 2008; 89: 24-32.
[29] Zacharaki EI, Wang SM, Chawla S, Yoo DS, Wolf R, Melhem ER and Davatzikos C. Classification of brain tumor type and grade using MRI texture and shape in a machine learning scheme. Magn Reson Med 2009; 62: 1609-1618.